International Journal of Heat and Mass Transfer 127 (2018) 332–344

Contents lists available at ScienceDirect

International Journal of Heat and Mass Transfer

journal homepage: www.elsevier.com/locate/ijhmt

# Thermoelectric currents and thermoelectric-magnetic effects in full-penetration laser beam welding of aluminum alloy with magnetic field support

Jicheng Chen [a,b], Yanhong Wei [a,*], Xiaohong Zhan [a], Cheng Gu [b], Xinyi Zhao [c]

[a] College of Material Science and Technology, Nanjing University of Aeronautics and Astronautics, Nanjing 211106, China
[b] Department of Materials Science and Engineering, The Ohio State University, Columbus, OH 43210, USA
[c] School of Materials Science and Engineering, Harbin Institute of Technology, Harbin 150001, China

ARTICLE INFO

*Article history:*
Received 21 June 2018
Received in revised form 31 July 2018
Accepted 2 August 2018

*Keywords:*
Thermoelectric currents
Thermoelectric-magnetic effects
Magnetically supported laser beam welding
Weld pool dynamics
Seam profile

ABSTRACT

Thermoelectric currents (TECs) caused by Seebeck effect were usually neglected in welding simulation. This paper characterizes the TECs and thermoelectric-magnetic phenomena during the magnetically supported laser beam welding (MSLBW) of thick aluminum (Al) alloy. The simulation is based on a computational fluid dynamic (CFD) model developed in three dimensions. The model considers multi-physical mechanisms including thermal transfer, solid–liquid (S/L) transition, molten metal convection, magneto-hydrodynamics (MHD) and Seebeck effect. The computed TEC distribution in laser welding pool highly depends on welding time and temperature gradient. The large current densities occur near the weld pool edge and the vectors are opposite at both side of S/L interface. The maximum TEC density obtained in the stabilized weld pool is $2.14 \times 10^6$ A/m$^2$, leading to a self-induced magnetic field of $2.27 \times 10^{-3}$ T and a Lorentz force of $2.62 \times 10^3$ N/m$^3$. The influences of TECs on weld pool dynamics are quite limited in LBW but notable in MSLBW. The inversion of MF direction leads to different Lorentz force distributions, weld pool dimensions and seam profiles. The simulation data agrees well with the experimental results.


## 1. Introduction

In a number of industry fields, the laser beam welding (LBW) process of thick aluminum (Al) alloys usually suffers from welding imperfections including humping pattern, spattering loss, porosity, etc. The high laser power input and low viscosity of Al are believed as primary factors as they always lead to dramatic molten metal convection and poor keyhole stability [1,2]. In recent years, magnetically supported laser beam welding (MSLBW) technology has got wide attention and rapid development as it can improve the welding quality through electromagnetic (EM) effects. Literatures published in recent years have involved the influences of magnetic fields (MFs) on weld profile [3,4], weld pool dynamics [1,2,5–8], plasma behavior [9,10] and alloying element dilution [11–13].

Many researchers worked on the melt flow and heat transfer behavior during MSLBW of thick/moderate thick Al alloys and considerable achievements were obtained with different magnetic support systems and parameters. Gatzen et al. [3] and Bachmann et al. [4,6] developed a thermal-flow-EM coupling model for MSLBW simulation and the results showed that the EM braking effect (Hartmann effect) occurred inside the weld pool under the function of an external static MF. The thermocapillary (Marangoni) convections were highly suppressed and the weld width was reduced. Chen et al. [8] revealed the melt flow pattern, heat transfer rate and the threshold effect of Hartmann effect during the full-penetration laser beam welding (LBW) of Al alloy under a longitudinal field. Gatzen et al. [11] studied the element dilution during MSLBW of AA99.5 with filler wire ($B_0$ = 160–360 mT, f = 10–20 Hz) and found that the populated silicon could be more uniformly distributed because of the periodically induced EM forces. Furthermore, Bachmann et al. [5] presented that during the laser welding of thick austenitic stainless steel, the drop-out of molten metal could be prevented by applying a horizontal oscillating field at the frequency of 1–10 kHz.

During the numerical solution of weld pool dynamics in presence of external MFs, apart from MHD phenomena, thermoelectric currents (TECs) and the corresponding thermoelectric-magnetic effects also deserve attention as they can induce additional volume forces and heat flux. The TECs generated in laser welding pool are attributed to Seebeck effect, which depends on temperature gradient $\nabla T$ and the absolute thermoelectric power S (Seebeck

* Corresponding author.
*E-mail address:* yhwei@nuaa.edu.cn (Y. Wei).

https://doi.org/10.1016/j.ijheatmasstransfer.2018.08.004
0017-9310/

coefficient) of material. In the early days, researchers focused more on the obvious Seebeck effect occurring during the welding of dissimilar metals. Paulini et al. [14] developed a two-dimensional irreversible thermodynamic model and calculated the TECs, symbiotic MF and Lorentz force in electron beam welding (EBW) and LBW. M. Ziolkowski and H. Brauer [15] extended the model into three dimensions. The Seebeck effect during EBW was estimated and the self-induced MF of TECs was proved to be the cause of electron beam deflection.

In fact, TECs can also be prominent under LBW condition for same metal because of high peak temperature (3000–5000 K) and high welding velocity which can lead to large temperature gradient in both liquid phase and solid phase. Kern et al. [1] pointed out that the existence of TECs in magnet-assisted welding pool might be responsible for the drastically different seam appearance when the MF direction was reversed. The measured thermoelectric voltage (TEV) based on a simple thermocouple system reached 50 μV. According to a subsequent simulation study conducted by Chen et al. [16], the TEC density up to $1 \times 10^7$ A/m$^2$ could be achieved during the deep-penetration laser welding of SS304 steel sheets, leading to the self-induced magnetic flux density of $1 \times 10^{-4}$ T and the Lorentz force larger than $1 \times 10^3$N/m$^3$. In comparison, the maximum electric current density and magnetic flux density caused by Hartmann effect were relatively lower, which were $1.8 \times 10^5$ A/m$^3$ and $5.5 \times 10^{-5}$ T, respectively ($B_0 = 0.2$ T) [8]. Consequently, for a more reliable description and prediction of weld pool information and seam formation in MSLBW process of Al alloys, the TEC effect should be considered in computations. Nevertheless, to the best of our knowledge, the relevant work has rarely been reported.

This paper presents the numerical solutions for transient TECs and thermoelectric-magnetic effects during the full-penetration MSLBW of 12-mm thick Al alloy plates. The proposed three-dimensional CFD model took into account the complex physical mechanisms including thermal transfer, phase transformation, molten convection, MHD effect and Seebeck effect. A well-tested equivalent keyhole model was adopted to enhance the computing efficiency for large welding penetration. The TECs, self-induced MF, Lorentz force and Joule heat were calculated and their influences on molten flow and heat transfer conditions and weld pool dimensions were comprehensively analyzed in comparison to reference cases. The simulation results were examined by literature data and experimentally determined seam profiles.

## 2. Mathematical modeling

As mentioned above, simulation on TECs and weld pool dynamics during MSLBW involves complex multi-physical mechanisms. To improve the calculation efficiency while holding the certain accuracy, several assumptions and simplifications were made in modeling process.

- The material is isotropic and the molten metal is Newtonian, incompressible and laminar.
- The weld pool surfaces are assumed to be flat.
- The shielding gas and its effect on liquid motion are neglected.
- The formation and dramatic fluctuation process of keyhole is neglected (taking about 0.03 s according to Pang et al. (2011, 2014) [17,18]). The keyhole is assumed in quasi-steady state with constant geometry from the very beginning. The evaporation and condensation processes are not calculated.
- The magnetic loss in surrounding atmosphere is negligible.
- No displacement electric currents exist inside or at the boundaries of computation domain [19].

The mass, momentum and energy conservation equations which govern the thermodynamics and kinetics of the weld pool under the approximations stated are listed as follows.

$$\nabla \cdot (\rho \vec{u}) = 0 \quad (1)$$

$$\frac{\partial}{\partial t}(\rho \vec{u}) + \rho \cdot (\vec{u} \cdot \nabla)\vec{u} = -\nabla p + \eta \nabla \cdot \left[(\nabla \vec{u} + \nabla \vec{u}^T) - \frac{2}{3}\nabla \cdot \vec{u} I\right] + \vec{S}_m \quad (2)$$

$$\frac{\partial}{\partial t}(\rho h) + \nabla \cdot (\rho h \vec{u}) = \nabla \cdot (k \nabla T) + S_h \quad (3)$$

Here, ρ, t, $\mathbf{u} = (u, v, w)$, p, η and T denote the mass density, welding time, velocity field, static pressure, dynamic viscosity and temperature, respectively. k and h in Eq. (3) denote the thermal conductivity and enthalpy. $\mathbf{S_m}$ and $S_h$ are the source terms for momentum and energy conservations.

$$\vec{S}_m = -\rho \vec{g} + \rho \vec{g} \beta (T - T_l) - c_1 \frac{(1 - f_l)^2}{f_l^3 + c_2}(\vec{u} - \vec{u}_0) + \vec{j} \times \vec{B} \quad (4)$$

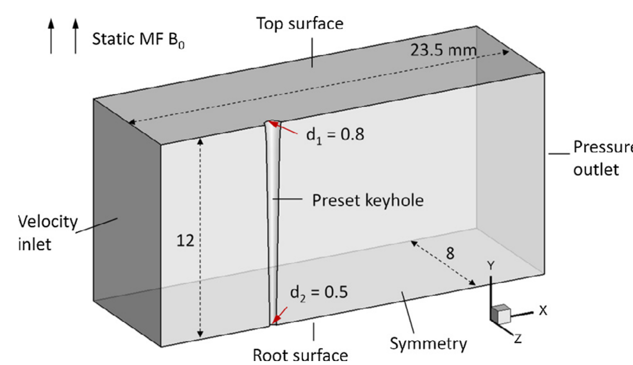


**Fig. 1.** Computational domain for the simulation of TECs and weld pool dynamics during MSLBW of Al alloy.

**Table 1**
Physical properties of 99.5 Al alloy used for simulation [3,23,24].

| Physical property | Symbol | Value | Unit |
|---|---|---|---|
| Mass density | ρ | 2380 | kg/m$^3$ |
| Thermal expansion coefficient | β | $2.8 \times 10^{-5}$ | 1/K |
| Solid temperature | $T_s$ | 930.35 | K |
| Liquid temperature | $T_l$ | 933.35 | K |
| Evaporation temperature | $T_v$ | 2700 | K |
| Heat conductivity ($T_l$) | λ | 91 | W/(m·K) |
| Heat capacity ($T_l$) | $C_p$ | 1180 | J/(kg·K) |
| Latent heat of fusion | $H_f$ | $3.97 \times 10^5$ | J/kg |
| Surface emissivity | ε | 0.062 | |
| Dynamic viscosity ($T_l$) | η | $1.1 \times 10^{-3}$ | Pa·s |
| Surface tension ($T_l$) | γ | 0.871 | N/m |
| Marangoni coefficient | ∂γ/∂T | $-1.55 \times 10^{-4}$ | N/(m·K) |
| Electric conductivity ($T_l$) | σ | $4.04 \times 10^6$ | S/m |
| Magnetic permeability | μ | $1.26 \times 10^{-6}$ | H/m |
| Liquid Seebeck coefficient | $S_l$ | $-2.25 \times 10^{-6}$ | V/K |
| Solid Seebeck coefficient | $S_s$ | $-1.5 \times 10^{-6}$ | V/K |

**Table 2**
Simulation cases for full-penetration MSLBW of 99.5 Al alloy.

| Case No. | External magnetic flux density $B_0$ (T) | Seebeck coefficient S (V/K) |
|---|---|---|
| 1 | 0 | 0 (no TECs) |
| 2 | 0 | $S_s/S_l$ |
| 3 | 0.2 | $S_s/S_l$ |
| 4 | −0.2 | $S_s/S_l$ |